Mapping the Plasma Potential in a Glass Box

Lori Scott, Naoki Ellis, Mudi Chen, Lorin S. Matthews, *Member, IEEE*, and Truell W. Hyde, *Member, IEEE*

***Abstract*— Modeling the dynamics of charged dust particles, confined in a glass box placed on the lower electrode of a GEC cell, requires that the interactions between the charged dust, plasma, and boundaries need to be accounted for in a self-consistent manner. The charged lower electrode affects the plasma conditions throughout the glass box, altering the electron and ion densities and temperatures within the plasma sheath. These plasma characteristics determine the charge collected on the walls of the surrounding glass box, the electric potential within the glass box, the dust charge, and ultimately the dynamics of the dust. This work describes the steps taken to build a simple model of the relationship between the plasma conditions and the potential within the box as well as the expected dust charge near the center of the box. The calculated potential and dust charge are used to construct acceleration maps for the dust, which are compared to experimentally measured acceleration of the dust within the box.**

***Index Terms*—Dusty plasmas, plasma sheaths**

I. Introduction

A complex plasma is an ionized gas containing ions, electrons and dust particles. The particles (as well as any plasma-facing surfaces) become charged by collecting electrons and ions from the plasma; this charge is usually negative due to the high thermal speed of the electrons.

In laboratory experiments, the dust can be levitated against the force of gravity in the vertical electric field of the plasma sheath above the lower electrode. When the potential energy of the particle interactions is large compared to the kinetic energy, the particles can organize into regular structures, such as two-dimensional plasma crystals [1], [2]. This allows the particles to be used to study the detailed physics of phase transitions [3]–[5], fluid motion in strongly coupled systems [6]–[8], and wave phenomena [9]–[12]. A benefit of dusty plasma systems is that the dynamics of the dust are characterized by easily-observable time and spatial scales.

In many experiments, conducted within a GEC rf reference cell [13], horizontal confinement of the dust is provided by a ring placed on top of or a shallow depression in the lower electrode. This confinement is weak in comparison to the strong confinement in the vertical direction provided by gravity and the sheath electric field. The resulting dust structures are planar, usually only consisting of a single to a few layers.

Increasing the confinement in the horizontal direction allows stable three-dimensional structures to be formed, such as coulomb balls, clusters, and extended vertical strings [14]–[20]. The equilibrium states of these structures strongly depend on the confinement conditions, controlled by the neutral gas pressure and the power delivered to the system [21].

Increased horizontal confinement can be achieved by placing a glass box on the lower electrode, the walls of which also become negatively charged. However, it is difficult to directly measure the conditions within the box as probes inserted into the plasma alter the local plasma conditions. Micrometer-sized dust particles, however, are small enough that they do not appreciably perturb the local plasma conditions [22]. Tracking the motion of the dust particles allows the forces that the plasma exert on the particles to be determined, providing a map of the plasma potential within the box [23]. Careful measurements have shown that the box creates a radially-symmetric confinement near the center of the box, which varies in strength depending on the height above the lower electrode. In addition, measurements have also shown that the box allows for an extended vertical region where the vertical acceleration of a charged particle exceeds the acceleration of gravity [22], [23].

One drawback of using the dust particles as probes is that it is difficult to measure a particle's charge independently of the electric field within the box. The particles' charge is usually assumed to be fixed, but is actually a function of the plasma conditions within the box. There are several methods to model the plasma conditions within a given geometry, including fluid models where plasma is treated as a continuous fluid [24], [25] and PIC models where the electrons and ions are treated as discrete particles [26]–[28]. However, these models usually take advantage of symmetry in the system to reduce the problem to two dimensions. A full treatment of a three-dimensional space takes much more computation time. Here we present a simplified model to approximate the effect that the box has on the local plasma conditions. The plasma conditions (electron and ion densities and temperatures) within the sheath above the lower electrode are first determined using a fluid model for varying system power and gas pressure. These plasma conditions are used to calculate the charge collected on the walls of the box. The sheath electric field at the center of the box is then modified by adding the electric field due to the charge on the box walls. The revised plasma conditions are also

Submitted for review September 30, 2018. This work was supported in part by the National Science Foundation under Grant PHY-1414523.

Lori C. Scott was with CASPER, Baylor University, Waco, TX 76798 USA. She is now with Auburn University, Auburn, AL 80305 USA (e-mail: lcs0044@tigermail.auburn.edu).

Naoki Ellis, Mudi Chen, Lorin S. Matthews, and Truell W. Hyde are all with CASPER, Baylor University, Waco, TX 76798 USA (e-mail: naoki_ellis@baylor.edu, mudi_chen@baylor.edu, lorin_matthews@baylor.edu, truell_hyde@baylor.edu).

used to determine the charge on dust particles confined within the box, allowing particle acceleration maps to be calculated, which can be compared with experimental measurements.

A description of the experimental setup and observations are given in Section II. The numerical model used to obtain the potential within the box is described Section III. The potential and electric fields calculated from the model are presented in Section IV and are compared to experimental measurements. A discussion of these results is found in Section V.

II. Experiment

A. Experimental Setup

Complex plasma experiments are carried out at CASPER in a Gaseous Electronic Conference rf reference cell filled with argon gas. The dust particles used are manufactured uniform spheres of melamine formaldehyde (MF) with a density of 1.154 g/cm^3 and diameter 8.89 μm. A glass box with inner dimensions 10.5 mm × 10.5 mm × 12.5 mm sits directly on the lower electrode of the cell, as shown in Fig. 1. Two cameras, one of each in the vertical and horizontal directions, are used to track the motion of the particles within the box at a rate of 500-1200 frames per second. The particles can be tracked from frame to frame to construct their trajectories, allowing the velocities and accelerations to be calculated.

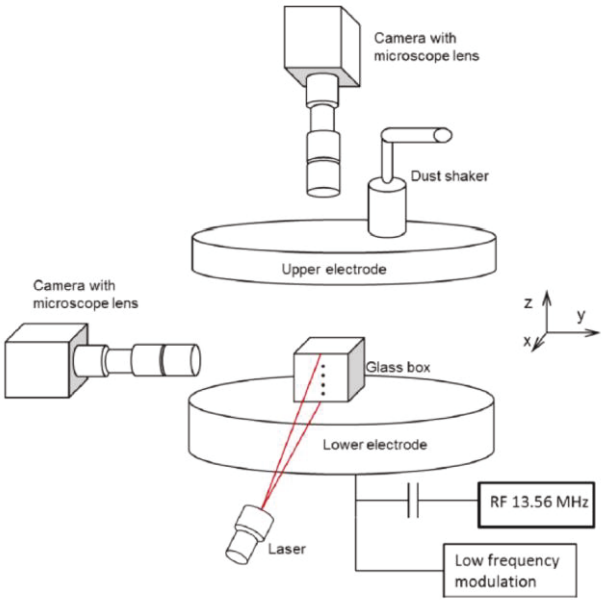

Figure 1. GEC rf reference cell schematic. The upper electrode is grounded and the lower electrode has a variable bias as needed. The glass box sits on the lower powered electrode and the two vertical and horizontal cameras track the motion of the dust particles within the box.

B. Observations

The total force acting on a particle consists of gravity, the confinement force from the electric field within the box, neutral gas drag, and the interaction force from other dust grains

$$\boldsymbol{F}_{total} = m\boldsymbol{g} + q\boldsymbol{E} - \beta\boldsymbol{v} + \boldsymbol{F}_{dd}. \quad (1)$$

Here m is the mass, q is the charge, and v is the velocity of the dust grain, β is the Epstein drag coefficient. Other forces, such as ion drag and thermophoresis are small compared to these forces and are not considered here. Equilibrium dust structures are primarily determined by the ratios of gravity, the confining electric fields in the horizontal and vertical directions, and the electrostatic interactions between the dust grains which are mediated by the surrounding plasma.

The confinement forces within the glass box lead to some unique dust particle structures which are rarely observed under other confinement conditions. These include a single vertically aligned dust particle chain and helical dust particle structures. The single vertical chain provides not only an ideal way to study the particle interaction and interaction with the vertical ion flow, but also an accurate and simple method to control the dust particle number. For example, once a vertical particle chain is formed, it is convenient to drop the lowest particle by slowly decreasing the system power. The helical structures undergo sharp phase transitions as the operating conditions (power and pressure) are changed, demonstrating the sensitivity of the stability of structures to the confinement [17], [21].

The change in levitation height of a single particle inside the glass box as the system power changes is also different than in other environments. With particle confinement provided by a cut-out or trench in the lower electrode, the levitation height always increases with increasing system power. Using the glass box, the height first decreases then increases while raising the power in a given range (this range is related to the pressure and the size of the dust particle). Other unique observed phenomena include turbulence, position-dependent response to changing system power (when decreasing the power, particles in some regions go up and in others go down) and particle motion which can best be explained by the presence of overlapping sheaths.

C. Mapping of the Electric Field

A dust particle is an ideal probe to investigate the plasma sheath due to its small perturbation to the plasma environment [29]. All coefficients in the equation of motion can be measured or calculated from gas parameters, with velocity and acceleration determined from the particle trajectories, allowing q**E** to be calculated. The details of this method are described in [23]. The mass of the dust particles can be calculated using the density and diameter as provided by the manufacturer. The gas drag coefficient β is defined as

$$\beta = \delta\frac{4\pi}{3}a^2\,\mathrm{N}m_n\,\bar{c}_n \quad (4)$$

where a is the radius of the dust particle, N is the neutral gas number density, m_n is the mass of the neutral gas atoms (Argon), and the coefficient δ accounts for the microscopic mechanism governing collisions between the gas atom and the surface of the dust particle. For MF particles and Argon gas, δ has been determined to be 1.44 as reported in Refs [30, 31]. Finally, $\bar{c}_n = \sqrt{8kT/\pi m_n}$ is the thermal speed of the neutral gas, where k is the Boltzmann constant and T is the temperature. Only trajectories where particles are far away from other dust particles are used in the analysis, allowing F_{dd} to be taken to be

negligible. By assuming a fixed charge on the dust particle, and averaging over many trajectories, the electric field can be mapped throughout the box. However, the charge on the dust particles is not constant, but instead varies with location due to the local plasma conditions [32]. An investigation of the electric field inside the glass box, using a numerical method to determine the charge on the box walls, the electric field due to the box, and the charge on the dust particles, will be introduced in the following and compared to the experimental results.

III. Numerical Model

It is evident that the charge on the walls of the box changes the potential within the box, altering the electric field both in the vertical and horizontal directions. To avoid the computational demands of a 3D PIC model to determine the plasma potential within the box, we use a two-dimensional plasma fluid model to determine the plasma parameters as a function of *z*, the height above the lower electrode. These plasma parameters are used to calculate local charging currents to the walls of the box, which are treated as a perfect insulator. The charge accumulated on the box walls is then used to calculate the contribution of the walls to the potential and electric field within the box.

A. Plasma Sheath Parameters

A basic assumption in this model is that the electron and ion densities within the plasma sheath determine the charge collection on the walls of the box. A self-consistent fluid model (a description of which can be found in [30]) is used to solve the equations for the electron and ion-fluid (in an argon discharge) as a function of the gas discharge parameters. These parameters include the gas pressure, the power delivered to the cell (as determined by the peak-to-peak amplitude of the driving potential) and the bias on the lower electrode. The output of the fluid model provides the spatially resolved plasma characteristics within CASPER's GEC rf reference cell, including the plasma potential $V(z)$, Debye length $\lambda_D(z)$, electron and ion densities $n_{e,i}(z)$, and electron temperature $T_e(z)$, where z is the height above the lower electrode [33].

B. Charging Calculation

Objects in a plasma environment become charged by collecting particles from the surrounding plasma. Using orbital motion-limited (OML) theory, the current density to a point t on a surface can be found by calculating the flux of charged particles to that point, given by

$$J_s(t) = n_s q_s \int_{v_{min}(t)}^{\infty} f_s(v_s) v_s^3 dv_s \times \iint \cos(\theta) d\Omega \quad (2)$$

where *s* denotes the plasma species (electron or ion) with number density *n* and charge *q*, *f(v)* is the distribution of velocities *v*, and θ is the angle between the surface normal and the incoming particle velocity. The lower limit in the integration $v_{min}(t) = \sqrt{2q_s V(t)/m_s}$ is the minimum velocity a plasma particle with mass m_s and the same polarity of charge as the surface must have to reach the surface with potential V. For plasma particles with the opposite polarity of charge, $v_{min}(t) = 0$. Assuming a Maxwellian velocity distribution for the electrons and ions with a given temperature T_s, the first integral can be calculated directly to give

$$\begin{aligned} J_{0s} \exp\left(-\frac{q_s V}{kT_s}\right), q_s V > 0 \\ J_{0s}\left(1 - \frac{q_s V}{kT_s}\right), q_s V < 0 \end{aligned} \quad (3)$$

where $J_{0s} = n_s q_s \sqrt{kT_s/2\pi m_s}$. The integration over the angles includes all directions for which the trajectories of the incoming plasma particles are not blocked, termed the Line of Sight (LOS) approximation [32].

The OML_LOS method is suitable to model the charge collected on any arbitrarily-shaped object, and here was adapted to model the charge collected on the interior surfaces of the glass box by dividing each face into $N \times M$ patches. The number of patches is determined by the Debye length in the plasma, with the patch dimension approximately equal to or smaller than λ_D. Three distinct types of surface patches were defined: the lower corners, where the open angles are one-octant of a sphere; the lower and interior edges of the panes, where the open angles are one quadrant of a sphere, and the remainder of the patches, where the open angles cover a hemisphere. These open angles were used to define the LOS_factor for the three types of patches. In the following work, $N \times M = 25 \times 30$, though it was determined that above this minimum resolution, the charge collected on the box walls was relatively independent of the number of patches.

C. Charge on the Box

To first approximation, the charge on the walls of the box is assumed to be determined by the electron and ion temperatures and densities within the sheath, established by the charged lower electrode. The quantities $n_i(z)$, $n_e(z)$, and $T_e(z)$ obtained from the fluid model were used to calculate the current density to each patch according to Eq (2). The ions are assumed to be at room temperature with $T_i = 298$ K. The lower limit of integration was set by the potential at the center of each patch, calculated from the sum of the potential due to all other patches on the box, the charge on the patch itself, and the potential due to the charge on the lower electrode

$$V_j = \sum_{i \neq j} V_{ij} + V_{self,j} + V_{sheath} \quad (4)$$

The potential due to the charge on the patch itself is calculated at the center of a square sheet of charge

$$V_{self} = \frac{\sigma}{2\pi\epsilon_0} l \log(17 + 12\sqrt{2}) \quad (5)$$

where σ is the charge density, and *l* is the length of the side of the patch. V_{ij} is the shielded Coulomb potential

$$V_{ij} = \frac{1}{4\pi\epsilon_0} \frac{q_i}{r_{ij}} \exp(-r_{ij}/\lambda_D(z)) \quad (6)$$

where q_i is the charge on the i^{th} patch, r_{ij} is the distance between patch i and patch j, and $\lambda_D(z)$ is the Debye length, obtained from the fluid model, as is V_{sheath}.
The current density is multiplied by the patch area to calculate the net electron and ion current to the center of each patch, and the net charge accumulated in the time step is determined. This process is iterated until equilibrium is reached, defined by a difference in total charge between the previous and current time step of less than 0.01%. The calculated charges on the walls of the box for a representative set of conditions are shown in Figure 2.

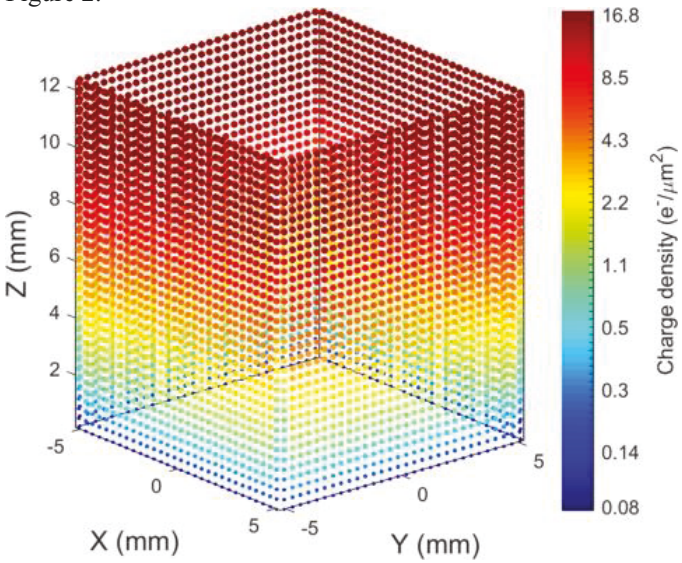

Fig. 2. (Color online) Equilibrium charge density on walls of the glass box with gas pressure 150 mTorr and driving potential 60 V_{PP}. Note the log scale for the color bar.

Note that the ion flow within the sheath is neglected in calculating the ion current, as the direction of ion flow is parallel to the box walls. The effect of neglecting this directed flow is discussed further in the conclusion.

IV. Mapping the Electric Field Inside the Box

The charge on the box walls was calculated for gas pressures P_g = 100, 150, 250, 350 mTorr and driving potentials, V_{pp} = 40-80 V, where the amplitude of the driving potential was measured peak-to-peak. The charges at each patch i on the box walls was used to calculate the potential at points A within the box $V_A = \sum_i V_{iA}$, using the Yukawa potential as in Eq. 6. To take into account the changing Debye length, the contribution from each patch charge to the potential was numerically integrated along the path connecting patch i to point A

$$V_{iA} = \frac{1}{4\pi\epsilon_0}\frac{q_i}{r_{iA}}\exp(-\Sigma_j \Delta r_j/\lambda_D(z)) \quad (7)$$

where Δr_j is a segment along the path with a length of one-third of the patch height. A representative map of the potential for vertical slice in the midplane of the box is shown in Fig. 3.

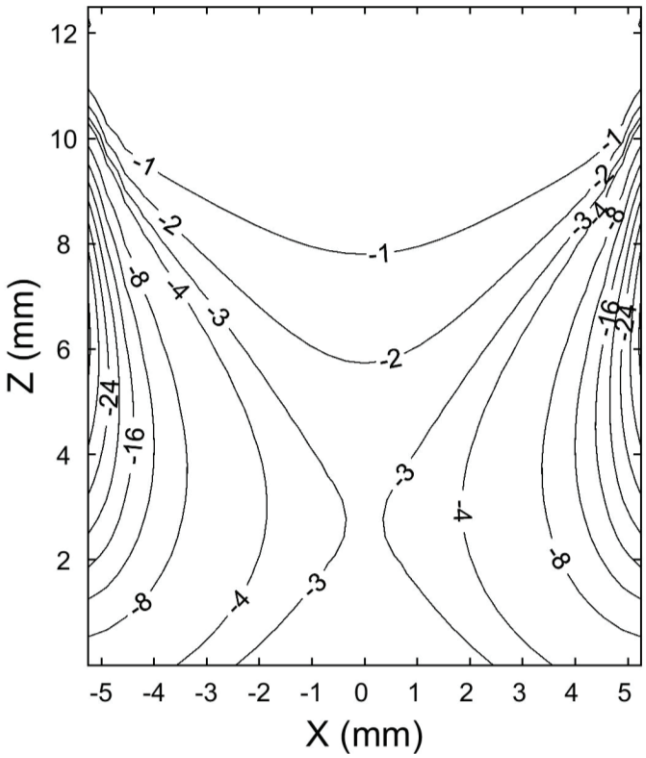

Figure 3. Potential (in Volts) within the glass box due to the charge on the walls. The slice is a vertical plane through the middle of the box. Plasma conditions are P_g = 150 mTorr, V_{PP} = 60 V.

The electric field within the box due to the charge on the walls was then calculated from $\vec{E} = -\nabla V$. The horizontal component of the electric is assumed to be solely due to the electric field of the box, while in the vertical direction the total electric field is due to the electric field of the sheath (obtained from the fluid model) plus the electric field of the box.
Under most experimental conditions, the particles are trapped in a small region very close to the centerline of the box. A comparison of the magnitude of the vertical electric field along the midline of the box due to the sheath alone and the sheath plus the box is shown in Figure 4a for a constant gas pressure, P_g = 150 mTorr, with varying driving potentials. As power increases, the magnitude and slope of the electric field increases. In the region where dust particles are stably trapped (2-8 mm above the lower electrode), the sheath electric field predicted by the fluid model is approximately linear. The addition of the box increases the magnitude of the electric field and flattens the slope slightly. The shift in the minimum of the potential makes the non-linearity in the sheath electric field an important factor in the stability of dust structure which span an appreciable vertical extent, such as a vertical chain. The effect becomes more pronounced at lower driving potentials (Figure 4a) and at lower pressures (Figure 4b), as the plasma density is reduced. The lower plasma density results in an increased shielding length, which allows the charge on the box walls to have a greater impact on the electric field within the box.

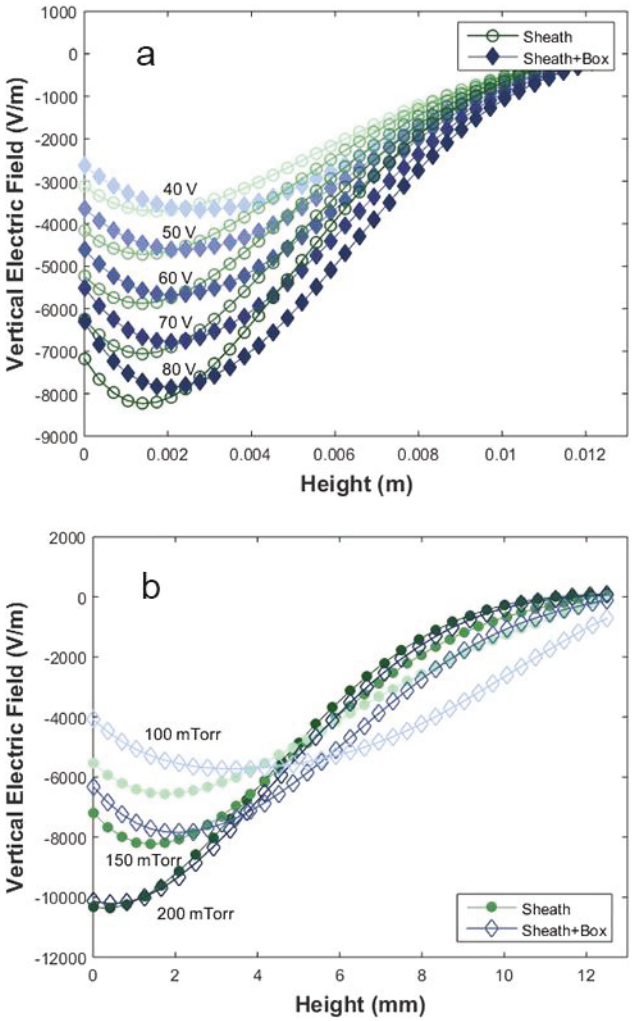

Fig. 4. (Color online) Vertical electric field along the midline of the box for (a) constant gas pressure, P = 150 mTorr, with varying driving potential and (b) constant driving potential V_{PP} = 60 V with varying pressure. The green circles denote the sheath electric field, the blue diamonds indicate the combined electric fields of the sheath and box.

The equilibrium charge on dust particles was also calculated for the same set of plasma conditions at various locations within the box, with the charge of a particle in the center of the box as a function of height above the lower electrode shown in Figure 5. The magnitude of the particle charge decreases as it approaches the lower electrode; however, as the vertical electric field increases in magnitude, there is an extended vertical region in which the electric force can balance gravity.

Acceleration maps can be constructed for the various plasma conditions (Figure 6 a,c) and compared with acceleration maps constructed from experimental data taken for similar plasma conditions as described in Section IIC (Figure 6 b,d). It should be noted that the numerically-derived acceleration map does not correctly account for the changing screening length as a particle approaches the box walls. However, the agreement along the midline of the box is fairly good. At lower pressures, the experimental and numerical acceleration maps show less agreement (Fig. 7). This indicates that the expanding sheaths from the box walls need to be treated in a manner which takes into account the non-linear nature of the sheath addition.

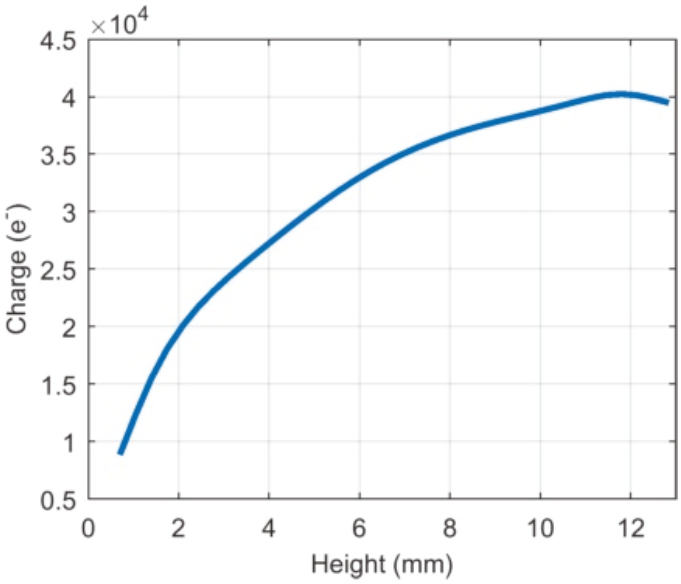

Figure 5. Particle charge vs height above lower electrode. Plasma conditions are P_g = 150 mTorr, V_{PP} = 60 V.

V. Discussion and Conclusion

A simple model was presented to calculate the charge collected on the walls of a glass box and determine how this charge alters the confining electric fields within the box. The comparison of the numerical and experimental results for the electric field inside the box indicate that for high powers the numerical model provides both qualitative and quantitative agreement in the vertical direction along the midline of the box, as shown in Fig. 6. Due to the changing plasma conditions in the vertical direction, there is an extended region where the vertical acceleration provided by the electric field exceeds that of gravity, which allows the stable trapping of extended vertical structures such as dust strings. The model does not take into account the formation of sheaths next to the box walls. At low power the sheaths above the lower electrode and from the box walls expand, and the overlapping sheaths add in a non-linear manner. In this case, the model, which assumes the linear addition of the electric fields, does not match the experimental results (Figure 7). Thus the electric field within the box is quite different from that in the sheath above the bare lower electrode.

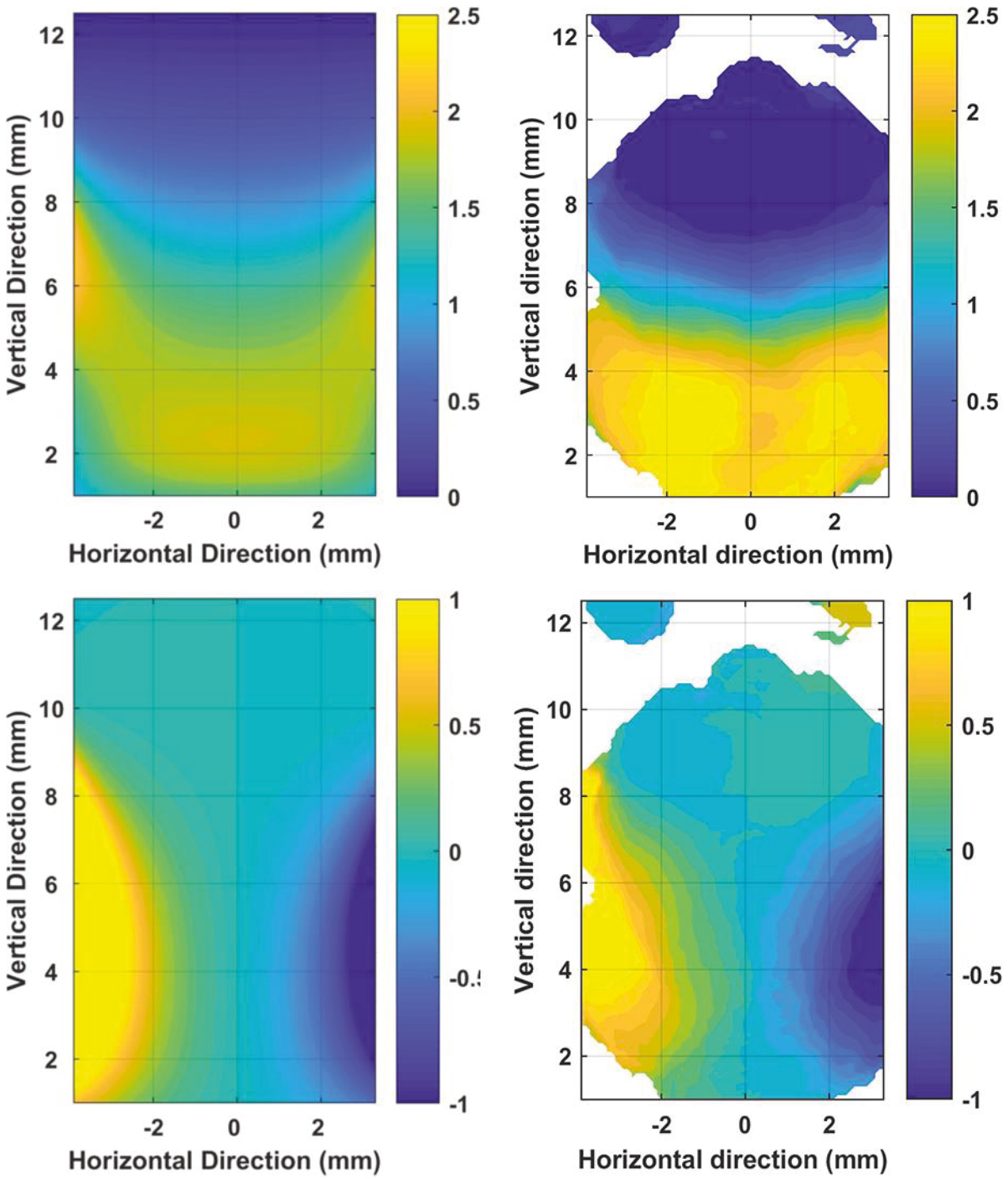

Figure 6. (Color online) Acceleration maps for charged dust particles within the box in the (top row) vertical and (bottom row) horizontal directions. The images on the left were generated by the numerical model (150 mTorr and 60 V_{pp}) and those on the right were measured by experiment (140 mTorr, driving potential 66 V_{pp}). The color bar gives the acceleration in units of g.

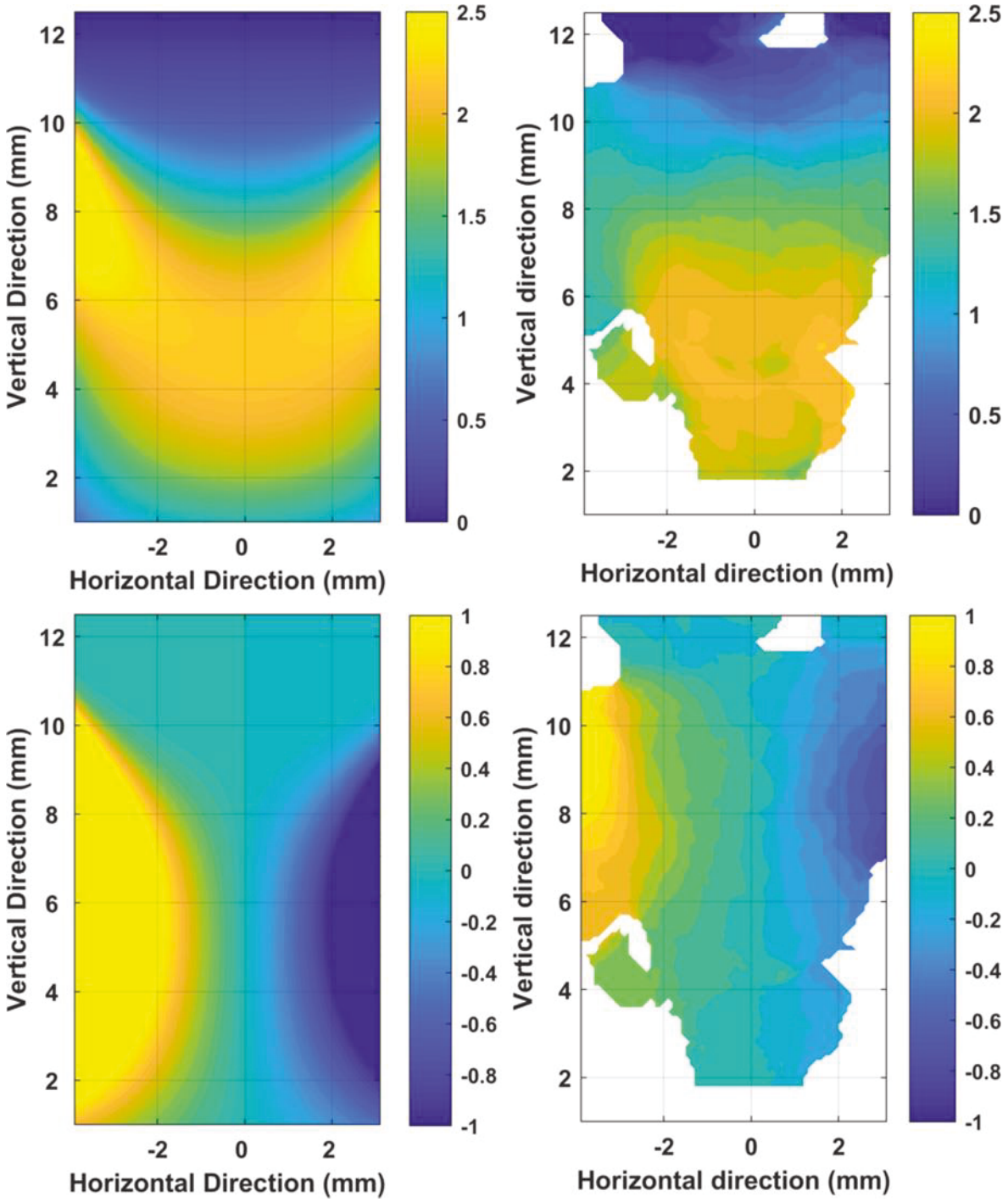

Figure 7. (Color online) Acceleration maps for charged dust particles within the box in the (top row) vertical and (bottom row) horizontal directions. The images on the left were generated by the numerical model (100 mTorr and 60 V_{pp}) and those on the right were measured by experiment (100 mTorr, driving potential 66 V_{pp}). The color bar gives the acceleration in units of g.

ACKNOWLEDGEMENTS

Support from NSF grant PHY-1414523 is gratefully acknowledged.

REFERENCES

[1] H. Thomas, G. E. Morfill, V. Demmel, J. Goree, B. Feuerbacher, and D. Möhlmann, "Plasma Crystal: Coulomb Crystallization in a Dusty Plasma," *Phys. Rev. Lett.*, vol. 73, no. 5, pp. 652–655, Aug. 1994.

[2] J. H. Chu and L. I, "Direct observation of Coulomb crystals and liquids in strongly coupled rf dusty plasmas," *Phys. Rev. Lett.*, vol. 72, no. 25, pp. 4009–4012, Jun. 1994.

[3] P. Hartmann *et al.*, "Crystallization Dynamics of a Single Layer Complex Plasma," *Phys. Rev. Lett.*, vol. 105, p. 115004, 2010.

[4] K. Qiao and T. W. Hyde, "Structural phase transitions and out-of-plane dust lattice instabilities in vertically confined plasma crystals," *Phys. Rev. E*, vol. 71, no. 2, p. 026406, Feb. 2005.

[5] A. V. Ivlev, U. Konopka, G. Morfill, and G. Joyce, "Melting of monolayer plasma crystals," *Phys. Rev. E*, vol. 68, no. 2, p. 026405, Aug. 2003.

[6] G. Kalman, M. Rosenberg, and H. E. DeWitt, "Collective Modes in Strongly Correlated Yukawa Liquids: Waves in Dusty Plasmas," *Phys. Rev. Lett.*, vol. 84, no. 26, pp. 6030–6033, Jun. 2000.

[7] V. Nosenko, A. V. Ivlev, and G. E. Morfill, "Microstructure of a Liquid Two-Dimensional Dusty Plasma under Shear," *Phys. Rev. Lett.*, vol. 108, no. 13, p. 135005, Mar. 2012.

[8] V. Nosenko, J. Goree, Z. W. Ma, and A. Piel, "Observation of Shear-Wave Mach Cones in a 2D Dusty-Plasma Crystal," *Phys. Rev. Lett.*, vol. 88, no. 13, p. 135001, Mar. 2002.

[9] V. V. Yaroshenko, A. V. Ivlev, and G. E. Morfill, "Coupled dust-lattice modes in complex plasmas," *Phys. Rev. E*, vol. 71, no. 4, p. 046405, Apr. 2005.

[10] N. N. Rao, P. K. Shukla, and M. Y. Yu, "Dust-acoustic waves in dusty plasmas," *Planet. Space Sci.*, vol. 38, no. 4, pp. 543–546, Apr. 1990.

[11] L. Couëdel, S. K. Zhdanov, A. V. Ivlev, V. Nosenko, H. M. Thomas, and G. E. Morfill, "Wave mode coupling due to plasma wakes in two-dimensional plasma crystals: In-depth view," *Phys. Plasmas 1994-Present*, vol. 18, no. 8, p. 083707, Aug. 2011.

[12] K. Qiao and T. W. Hyde, "Dispersion properties of the out-of-plane transverse wave in a two-dimensional Coulomb crystal," *Phys. Rev. E*, vol. 68, no. 4, p. 046403, Oct. 2003.

[13] P. J. Hargis *et al.*, "The Gaseous Electronics Conference radio-frequency reference cell: A defined parallel-plate radio-frequency system for experimental and theoretical studies of plasma-processing discharges," *Rev. Sci. Instrum.*, vol. 65, no. 1, p. 140, Jan. 1994.

[14] O. Arp, D. Block, A. Piel, and A. Melzer, "Dust Coulomb Balls: Three-Dimensional Plasma Crystals," *Phys. Rev. Lett.*, vol. 93, no. 16, p. 165004, Oct. 2004.

[15] P. Ludwig, H. Kählert, and M. Bonitz, "Ion-streaming induced order transition in three-dimensional dust clusters," *Plasma Phys. Control. Fusion*, vol. 54, no. 4, p. 045011, Apr. 2012.

[16] A. Melzer, A. Schella, and M. Mulsow, "Nonequilibrium finite dust clusters: Connecting normal modes and wakefields," *Phys. Rev. E*, vol. 89, no. 1, p. 013109, Jan. 2014.

[17] T. W. Hyde, J. Kong, and L. S. Matthews, "Helical structures in vertically aligned dust particle chains in a complex plasma," *Phys. Rev. E*, vol. 87, no. 5, p. 053106, May 2013.

[18] T. Kamimura and O. Ishihara, "Coulomb double helical structure," *Phys. Rev. E*, vol. 85, no. 1, p. 016406, Jan. 2012.

[19] J. Kong, T. W. Hyde, L. Matthews, K. Qiao, Z. Zhang, and A. Douglass, "One-dimensional vertical dust strings in a glass box," *Phys. Rev. E*, vol. 84, no. 1, p. 016411, Jul. 2011.

[20] L. G. D'yachkov, M. I. Myasnikov, O. F. Petrov, T. W. Hyde, J. Kong, and L. Matthews, "Two-dimensional and three-dimensional Coulomb clusters in parabolic traps," *Phys. Plasmas 1994-Present*, vol. 21, no. 9, p. 093702, Sep. 2014.

[21] J. Kong, K. Qiao, L. S. Matthews, and T. W. Hyde, "Interaction force in a vertical dust chain inside a glass box," *Phys. Rev. E*, vol. 90, no. 1, p. 013107, Jul. 2014.

[22] P. Hartmann, A. Z. Kovács, J. C. Reyes, L. S. Matthews, and T. W. Hyde, "Dust as probe for horizontal field distribution in low pressure gas discharges," *Plasma Sources Sci. Technol.*, vol. 23, no. 4, p. 045008, Aug. 2014.

[23] M. Chen, M. Dropmann, B. Zhang, L. S. Matthews, and T. W. Hyde, "Ion-wake Field inside a Glass Box," *Phys. Rev. E*, vol. 94, no. 3, Sep. 2016.

[24] V. Land and W. J. Goedheer, "Effect of large-angle scattering, ion flow speed and ion-neutral collisions on dust transport under microgravity conditions," *New J. Phys.*, vol. 8, pp. 8–8, Jan. 2006.

[25] V. Land, E. Shen, B. Smith, L. Matthews, and T. Hyde, "Experimental and computational characterization of a modified GEC cell for dusty plasma experiments," *New J. Phys.*, vol. 11, no. 6, p. 063024, Jun. 2009.

[26] W. J. Miloch, "Numerical simulations of dust charging and wakefield effects," *J. Plasma Phys.*, vol. 80, no. 6, pp. 795–801, Dec. 2014.

[27] I. H. Hutchinson, "Ion collection by a sphere in a flowing plasma: I. Quasineutral," *Plasma Phys. Control. Fusion*, vol. 44, no. 9, p. 1953, 2002.

[28] I. H. Hutchinson, "Ion collection by a sphere in a flowing plasma: 3. Floating potential and drag force," *Plasma Phys. Control. Fusion*, vol. 47, no. 1, p. 71, Jan. 2005.

[29] A. Douglass, V. Land, K. Qiao, L. Matthews, and T. Hyde, "Using dust as probes to determine sheath extent and structure," *J. Plasma Phys.*, vol. 82, no. 4, Aug. 2016.

[30] V. Land, L. S. Matthews, T. W. Hyde, and D. Bolser, "Fluid modeling of void closure in microgravity noble gas complex plasmas," *Phys. Rev. E*, vol. 81, no. 5, p. 056402, May 2010.

[31] B. Liu, J. Goree, V. Nosenko, and L. Boufendi, "Radiation pressure and gas drag forces on a melamine-formaldehyde microsphere in a dusty plasma," *Phys. Plasmas*, vol. 10, no. 1, pp. 9–20, Dec. 2002.

[32] A. Douglass, V. Land, L. Matthews, and T. Hyde, "Dust particle charge in plasma with ion flow and electron depletion near plasma boundaries," *Phys. Plasmas*, vol. 18, no. 8, pp. 083706-083706–6, Aug. 2011.

[33] A. Douglass, V. Land, K. Qiao, L. Matthews, and T. Hyde, "Determination of the levitation limits of dust particles within the sheath in complex plasma experiments," *Phys. Plasmas*, vol. 19, no. 1, pp. 013707-013707–8, Jan. 2012.

[34] L. S. Matthews, V. Land, and T. W. Hyde, "Charging and Coagulation of Dust in Protoplanetary Plasma Environments," *Astrophys. J.*, vol. 744, no. 1, p. 8, Jan. 2012.

Lori Scott was born in Duluth, MN in 1994. She received her B.S. degree from Baylor University, Waco, TX in May 2016. While at Baylor, she was a member of the 2015 Center for Astrophysics, Space Physics, & Engineering Research (CASPER) summer Undergraduate Research Fellows program at Baylor University, Waco, TX. She is a currently a Ph.D. candidate at Auburn University, Auburn, AL, where she is a member of the Magnetized Plasma Research Laboratory (MPRL) at Auburn with a research focus on complex (dusty) plasmas in a microgravity environment.

Naoki Ellis is currently an undergraduate student at Baylor University in Waco, TX, and his major field of study is physics. He was a Fellow in the 2017 Center for Astrophysics, Space Physics, & Engineering Research (CASPER) summer Undergraduate Research program at Baylor University, Waco, TX.

Mudi Chen received the B.S. and Master degrees in applied physics from the University of Science and Technology of China, Hefei, China, in 2007 and 2010, respectively. He is currently a Ph.D. candidate in plasma physics at Baylor University, Waco, TX, USA. His research interests include particle–particle interactions, diagnosing the plasma sheath, and the ion wake effect in the complex plasma.

Lorin S. Matthews received the B.S. and the Ph.D. degrees in physics from Baylor University in Waco, TX, in 1994 and 1998, respectively. She is an Associate Professor in the Physics Department at Baylor University and Associate Director of the Center for Astrophysics, Space Physics, and Engineering Research (CASPER). Previously, she worked at Raytheon Aircraft Integration Systems as the Lead Vibroacoustics Engineer on NASA's SOFIA (Stratospheric Observatory for Infrared Astronomy) project.

Truell W. Hyde was born in Lubbock, Texas. He received the B.S. in physics and mathematics from Southern Nazarene University in l978 and the Ph.D. in theoretical physics from Baylor University in 1988. He is currently at Baylor University where he is the Director of the Center for Astrophysics, Space Physics & Engineering Research (CASPER), a Professor of physics and the Vice Provost for Research for the University. His research interests include space physics, shock physics and waves and nonlinear phenomena in complex (dusty) plasmas.